

10 to 70% methanol in 50 mM  $\text{KH}_2\text{PO}_4$  over 25 min, 10 ml/min, monitor at 380 nm). Next, the HPLC-purified mixture was desalted on the same column (methanol was removed on a rotary evaporator, and the sample loaded in  $\text{H}_2\text{O}$  and eluted with 90% methanol) and lyophilized, yielding the purified Nvoc-aa-S-CoA (40 to 80% yield) as a yellow solid. For preparation of the deprotected aa-S-CoAs, the solution of Nvoc-aa-S-CoA collected from the HPLC purification was directly photolyzed (4°C, 350 nm, 1 hour), purified by HPLC again (four injections, TSK gel C18 5×20 cm, 5  $\mu\text{m}$ , 120 Å, 0 to 40% methanol in 50 mM  $\text{KH}_2\text{PO}_4$  over 25 min, 10 ml/min, monitor at 280 nm), and desalted. After removal of methanol on a rotary evaporator, the sample was lyophilized to give the aa-S-CoA (50 to 80% yield) as a white solid.

10. L. E. N. Quadri et al., *Biochemistry* **37**, 1585 (1998).

11. PheATE, PheAT, PheTE, and PheT are deletion mutants or derivatives of the phenylalanine (Phe)-activating enzyme GrsA, containing combinations of the A domain, the T domain, and the epimerization (E) domain. ProCAT is the recombinant first module of TycB, containing a proline (Pro)-activating A domain, a T domain, and the upstream C domain.

12. The construction of the expression plasmids pPheATE and pProCAT was described previously (15). We amplified the insert of the His-tagged T domain clone pPheT (PheATE residues 523 to 613) from chromosomal DNA of *Bacillus brevis* (American Type Culture Collection 9999) with Turbo-Pfu polymerase (Stratagene) using the manufacturer's protocol and the following 5'-modified oligonucleotides: 5'-Nco I, 5'-ATACCATGGCGGAACCTGATTTAACTTCCGG-3', and 3'-Bgl II, 5'-ATAAGA TCTTTACTATCTTTATATAATGAACC-3'. The amplified DNA was purified, digested with Nco I and Bgl II, and ligated into the expression vector pQE60. DNA sequencing of pPheT and mass spectrometric analysis of the purified gene product revealed two modifications: a His<sup>34</sup> → Gln substitution caused by a CAT-to-CAA transversion, and posttranslational removal of the NH<sub>2</sub>-terminal methionine. Neither modification interfered with the apo-to-holo conversion of this T domain. The enzymatic integrity of all proteins was confirmed in the adenosine triphosphate (ATP)-pyrophosphate exchange and thioester formation assays (15). Apo-to-holo conversion of the T domain was verified by phosphopantetheinylation with [<sup>3</sup>H]CoASH and Sfp (10). A derivative of pPheATE, featuring a cleavable His tag, was obtained by recloning the 3.3-kb *grsA* fragment from pPheATE into pET28b. After expression and affinity purification with Ni<sup>2+</sup>-nitrilotriacetic acid resin, the pure protein was dialyzed against MES buffer, pH 7.0, and cleaved with thrombin. The protein solution was gel-filtered (P-30 Micro Bio-Spin columns; Bio-Rad) and applied to a Ni<sup>2+</sup>-nitrilotriacetic acid column, providing PheATE in the flow-through, which was then used for the described [<sup>3</sup>H]Phe-transfer assay. His-tagged and untagged PheATE are enzymatically identical.

13. Phosphopantetheinylations were performed in MES buffer pH 7.0 (50 mM MES, 100 mM NaCl, 10 mM MgCl<sub>2</sub>, and 1 mM EDTA) containing 25  $\mu\text{M}$  PheT and 2 to 100  $\mu\text{M}$  CoASH (or derivative). Reactions were initiated by the addition of 25 nM Sfp. At various time points, 100- $\mu\text{l}$  samples were taken and quenched with 10  $\mu\text{l}$  of EDTA (0.5 M). After addition of 25  $\mu\text{l}$  of sample buffer [40% glycerol (v/v), 20%  $\beta$ -mercaptoethanol (v/v) and bromophenol blue (5 mg/l)], 25- $\mu\text{l}$  samples were applied to native tris-tricine gels [H. Schagger and G. von Jagow, *Anal. Biochem.* **166**, 368 (1987)]. The  $\beta$ -mercaptoethanol hydrolyzed the aa-S-Ppant-T thioesters, resulting in conversion to holo T domains, thus eliminating errors in quantitation due to partial hydrolysis during separation. Coomassie-stained gels were analyzed densitometrically with NIH Image 1.6.1 software. For larger peptide synthetase fragments, a spectrophotometric assay was used. Single reactions (100  $\mu\text{l}$ ) containing 25  $\mu\text{M}$  T domain (15  $\mu\text{M}$  PheAT or PheTE) and 2 to 100  $\mu\text{M}$  Nvoc-D-Phe-S-CoA were run with or without Sfp for 45 min, quenched by addition of 10  $\mu\text{l}$  of EDTA (0.5 M), gel-filtered (P-6 Micro Bio-Spin Columns; Bio-Rad), and analyzed for absorbance at 350 nm. The values reported were normalized for protein content at 220 nm, and the reliability of the method

was confirmed by comparison with identical samples in the PAGE assay. Kinetic constants are as follows (P, PAGE assay; A, absorbance assay). For PheT acceptor: CoASH (P,  $k_{\text{cat}} = 14 \text{ min}^{-1}$ ;  $K_m = 14 \mu\text{M}$ ;  $k_{\text{cat}}/K_m = 1 \mu\text{M}^{-1} \text{ min}^{-1}$ ), Nvoc-D-Ala-S-CoA (P, 20:27:0.7), Nvoc-L-Ala-S-CoA (P, 18:20:0.9), Nvoc-D-Phe-S-CoA (P, 18:13:1.4) and (A, 16:9:1.8), D-Phe-S-CoA (P, 15:8:1.9), Nvoc-L-Phe-S-CoA (P, 17:17:1), L-Phe-S-CoA (P, 22:19:1.2). For PheAT acceptor: Nvoc-D-Phe-S-CoA (A, 17:16:1.1). For PheTE acceptor: Nvoc-D-Phe-S-CoA (A, 15:16:0.9).

14. P. Belshaw, C. Walsh, T. Stachelhaus, data not shown.

15. T. Stachelhaus, H. D. Mootz, V. Bergendahl, M. A. Marahiel, *J. Biol. Chem.* **273**, 22773 (1998).

16. Introduction of aa-S-Ppant from Nvoc-aa-S-CoAs into PheATE and ProCAT was accomplished as follows: 2.5  $\mu\text{M}$  apo enzymes were incubated for 30 min at 37°C with 25  $\mu\text{M}$  Nvoc-aa-S-CoA, 50 nM Sfp (10), and 5% dimethyl sulfoxide (v/v) in MES buffer pH 7.0. The reaction mixtures were gel-filtered (P-6 Micro Bio-Spin Columns; Bio-Rad) to remove the excess of CoA derivatives and to exchange the MES buffer pH 8.0. Deprotection of the Nvoc group was performed in an ultraviolet reactor (maximum wavelength  $\lambda_{\text{max}} = 350 \text{ nm}$ , distance = 50 to 100 mm; Rayonet Photochemical Reactor, Branford, CT) for 15 min on ice, and the aminoacylated proteins were instantly used in condensation reactions. To ensure a complete aminoacylation of the second module, we incubated the respective holo enzyme with its cognate, radiolabeled substrate: 1  $\mu\text{M}$  holo enzyme was incubated at 37°C in MES buffer, pH 8.0, containing 2 mM ATP and 4.4  $\mu\text{M}$  L-[4-<sup>3</sup>H]Phe (27.0 Ci/mmol) or 4.8  $\mu\text{M}$  L-[5-<sup>3</sup>H]Pro (24.7 Ci/mmol). Simultaneously, a 1  $\mu\text{M}$  solution of the other aminoacylated module in MES buffer, pH 8.0, was also incubated at 37°C. After 3 min, the condensation reaction was initiated by combining equal volumes of both solutions. At

various time points, 100- $\mu\text{l}$  samples were taken and immediately quenched by the addition of 0.8 ml of 10% trichloroacetic acid (TCA) (w/v) and 20  $\mu\text{l}$  of bovine serum albumin (BSA) solution [2% (w/v)]. The TCA precipitate was washed once with 0.5 ml of 10% TCA (w/v), and the acid-stable label was quantified by LSC. The supernatants were extracted with 0.5 ml of butanol/chloroform [4:1; (v/v)], the organic layers were washed once with 0.5 ml of 0.1 M NaCl, and the amount of extractable label (DKP) was quantified by LSC (15).

17. The rate of formation of the dipeptidyl-S-T domain intermediate is about three to four times as fast as the subsequent release of the corresponding DKP product. For the wild-type system, the following rates were determined: 1.8  $\text{min}^{-1}$  for the formation of D-Phe-L-Pro-S-Ppant and 0.5  $\text{min}^{-1}$  for DKP release. The donor-site assay only assesses the slower DKP formation, so no argument can be made about possible rate differences for the formation of various aa-L-Pro dipeptide intermediates, except that they are no slower than 0.4 to 0.5  $\text{min}^{-1}$ .

18. V. de Crécy-Lagard, P. Marliere, W. Saurin, *C. R. Acad. Sci. Ser. III Sci. Vie* **318**, 927 (1995).

19. V. de Crécy-Lagard et al., *J. Bacteriol.* **179**, 705 (1997).

20. T. Stein et al., *J. Biol. Chem.* **271**, 15428 (1996); J. Vater, et al., *J. Prot. Chem.* **16**, 557 (1997).

21. H. Jakubowski, *Biochemistry* **37**, 5147 (1998).

22. U. Keller, *J. Biol. Chem.* **262**, 5852 (1987).

23. Supported in part by NIH grant GM20011, an European Molecular Biology Organization fellowship (T.S.) and a fellowship from the Jane Coffin Childs Memorial Fund for Medical Research (P.J.B.).

19 January 1999; accepted 16 March 1999

## Functional Arteries Grown in Vitro

L. E. Niklason,<sup>1\*</sup> J. Gao,<sup>2</sup> W. M. Abbott,<sup>3</sup> K. K. Hirschi,<sup>5</sup> S. Houser,<sup>4</sup> R. Marini,<sup>6</sup> R. Langer<sup>7</sup>

A tissue engineering approach was developed to produce arbitrary lengths of vascular graft material from smooth muscle and endothelial cells that were derived from a biopsy of vascular tissue. Bovine vessels cultured under pulsatile conditions had rupture strengths greater than 2000 millimeters of mercury, suture retention strengths of up to 90 grams, and collagen contents of up to 50 percent. Cultured vessels also showed contractile responses to pharmacological agents and contained smooth muscle cells that displayed markers of differentiation such as calponin and myosin heavy chains. Tissue-engineered arteries were implanted in miniature swine, with patency documented up to 24 days by digital angiography.

Atherosclerotic vascular disease, in the form of coronary artery and peripheral vascular disease, is the largest cause of mortality in the

United States (1). Surgical mainstays of therapy for affected vessels less than 6 mm in diameter include bypass grafting with autologous veins or arteries (2); however, adequate tissue for bypass conduits is lacking in many patients. Artificial materials, when used to bypass arteries that are less than 6 mm in diameter, have thrombosis rates greater than 40% after 6 months (3). Although novel approaches for producing small-caliber arterial grafts have been developed, problems with mechanical properties (4) or the utilization of neonatal cells (5) have heretofore prevented clinical implementation.

We report here the development of tech-

<sup>1</sup>Departments of Anesthesia and Biomedical Engineering, Duke University, Durham, NC 27710, USA. <sup>2</sup>Department of Biomedical Engineering, Case Western Reserve University, Cleveland, OH 44106, USA. <sup>3</sup>Department of Surgery, <sup>4</sup>Department of Pathology, Massachusetts General Hospital, Boston, MA 02114, USA. <sup>5</sup>Children's Nutrition Research Center, Baylor College of Medicine, Houston, TX 77030, USA. <sup>6</sup>Department of Comparative Medicine, <sup>7</sup>Department of Chemical Engineering, Massachusetts Institute of Technology, Cambridge, MA 02139, USA.

\*To whom correspondence should be addressed. E-mail: nikla001@mc.duke.edu

## REPORTS

niques to produce small-caliber autologous arteries in vitro from vascular cells grown on a biodegradable polymer matrix, by means of a pulsatile perfusion system for vessel culture. Ideal biological grafts should possess a confluent endothelium and differentiated, quiescent, smooth muscle cells (SMCs), as well as sufficient mechanical integrity and elastic moduli to allow suture retention and tolerance of systemic arterial pressures. Because vascular cells are exposed to pulsatile physical forces during most of vasculogenesis (6) and throughout life, we hypothesized

that the development of arteries in the laboratory would be facilitated by the application of pulsatile physical stress to cultured vascular cells (7, 8).

The biomimetic system we used for vessel culture is composed of bioreactors containing engineered vessels assembled in a parallel flow system (Fig. 1). In initial experiments, a suspension of cultured SMCs isolated from the medial layer of bovine aorta (9) was pipetted onto tubular biodegradable polyglycolic acid (PGA) scaffolds that were secured in bioreactors (10). The surface of the PGA

scaffolds was chemically modified with sodium hydroxide (11), which caused ester hydrolysis on the surface of the fibers, leading to increased hydrophilicity, increased adsorption of serum proteins, and improved SMC attachment. After an initial SMC seeding period of 30 min, the bioreactors were filled with medium and the SMCs were cultured under conditions of pulsatile radial stress for 8 weeks (Fig. 1). Control vessels were cultured without pulsatile radial stress under otherwise identical conditions.

After 8 weeks of culture, the gross appearance of the vessels was identical to that of native arteries. Histologic examination of pulsed vessels revealed that SMCs migrated inward to envelop PGA fragments in the vessel wall, resulting in a smooth luminal surface onto which bovine aortic endothelial cells (ECs) (12) could easily be seeded (Fig. 2, A and B). In contrast, nonpulsed controls exhibited no such inward SMC migration through the polymer scaffold (Fig. 2, C and D) and possessed an uneven layer of polymer fragments in the vessel lumen. Thus, vessels cultured under pulsatile conditions had a histologic appearance more similar to that of native arteries.

On the basis of these observations of vessel lumen morphology, we applied bovine aortic EC layers to vessels that had been cultured for 8 weeks under pulsatile conditions. After EC seeding, continuous perfusion of the vessel lumens was instituted for the final 3 days of culture. After 3 days, the presence of an endothelial layer on the luminal surface was confirmed by scanning electron microscopy (Fig. 2G) and by staining for von Willebrand factor and platelet endothelial cell adhesion molecule (PECAM, Fig. 2H).

The mechanical properties of native arteries rely on contractile SMCs, collagen, and elastin. Models of the wall mechanics of muscular arteries have shown that recruited bundles of collagen fibers contribute most of the incremen-

**Fig 1.** Biomimetic system for vessel culture. Non-cross-linked PGA mesh scaffolds were sewn into tubular form with 6-0 uncoated Dexon suture and were connected in bioreactors and sterilized by ethylene oxide. Scaffolds were seeded with 1 to 2 ml of a suspension of aortic SMCs at  $5 \times 10^6$  cells/ml. After seeding, bioreactors were filled with Dulbecco's modified Eagle's medium (DMEM) (200 ml per vessel), supplemented with 20% fetal bovine serum, penicillin G (100 U/ml), 5 mM HEPES, ascorbic acid (0.05 mg/ml),  $\text{CuSO}_4$  (3 ng/ml), proline, alanine, and glycine. The bioreactors and fluid reservoir were fitted to provide gas exchange, and buffer flowed through highly distensible silicone tubing inserted through the vessel lumen. The compliance chamber consisted of a 300-ml plastic reservoir that minimized the transmission of high-frequency vibrations to the bioreactors. Pulsatile radial stress was applied to the vessels at 165 beats per minute and 5% radial distention (strain). These conditions were chosen to approximate fetal development in large mammals. After 8 weeks, the silicone tubing was removed, and the flow of the medium was applied directly through the cultured vessel. To produce an endothelial layer, an EC suspension of  $3 \times 10^6$  cells/ml in DMEM was injected into the lumen, and the cells were allowed to adhere for 90 min. Luminal flow rate was then gradually increased from 0.033 to 0.1 ml/s over 3 days of culture, with corresponding shear stresses at the vessel wall of  $1 \times 10^{-2}$  N/m<sup>2</sup> to  $3 \times 10^{-2}$  N/m<sup>2</sup>. SMCs and ECs used for vessel culture were all below passage five at the time of seeding.

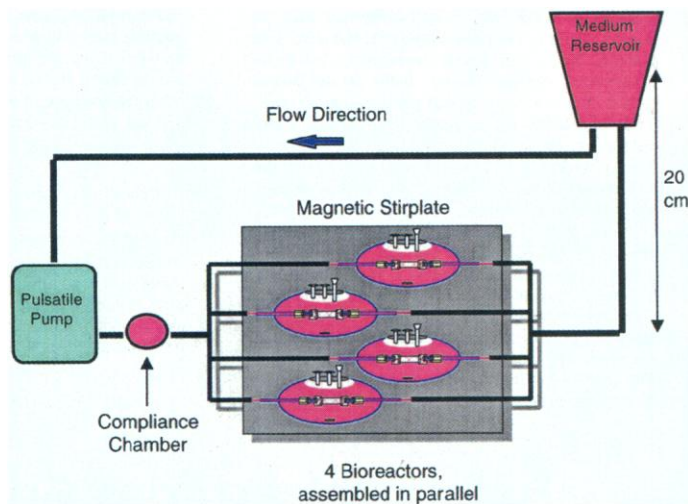
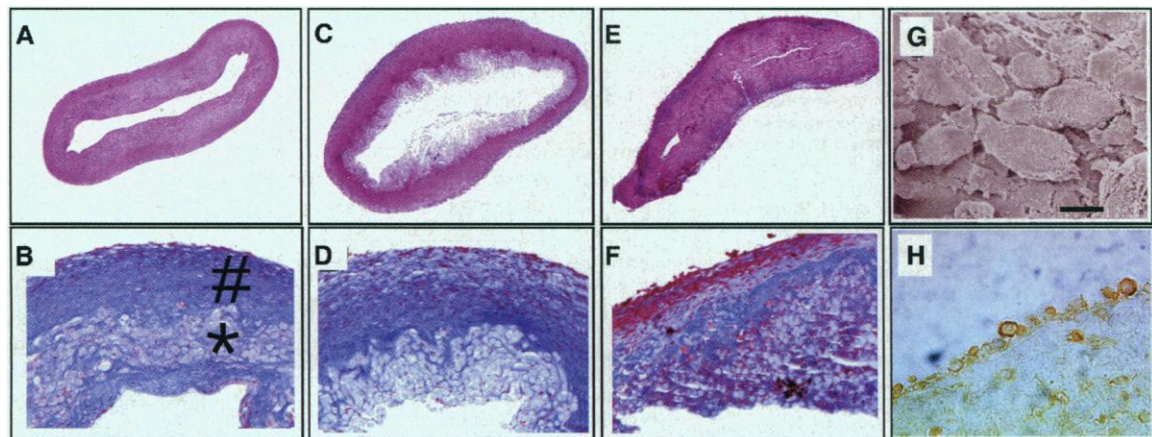


**Fig 2.** Histology of engineered vessels. (A and B) Pulsed vessel cultured for 8 weeks. (A) Verhoff's elastin stain [original magnification (orig. mag.)  $\times 20$ ]. (B) Masson's trichrome stain; collagen stains blue (orig. mag.  $\times 100$ ). Number sign indicates the dense cellular region; asterisk indicates the polymer region. (C and D) Non-pulsed vessel cultured for 8 weeks. (C) Verhoff's stain (orig. mag.  $\times 20$ ). (D) Masson's stain (orig. mag.  $100\times$ ). (E and F) Pulsed vessel without medium supplementation. (E) Verhoff's stain (orig. mag.  $\times 20$ ). (F) Masson's stain (orig. mag.  $\times 100$ ). (G) Scanning electron microscopy of the endothelial cell layer in an engineered vessel; cells are less confluent and more rounded than those of the arterial endothelium. Scale bar, 10  $\mu\text{m}$ . (H) Immunoperoxidase staining for PECAM antigen reveals an EC monolayer on the vessel lumen. Nonspecific staining of polymer fragments is apparent deeper in the vessel wall (orig. mag.  $\times 1000$ ).



## REPORTS

tal elastic modulus at intraluminal pressures above 100 to 200 millimeters of mercury (mm Hg) (13, 14). The mechanical properties of the engineered vessels ultimately derive from the SMCs and the extracellular matrix proteins they produce, because the PGA scaffold becomes fragmented and degrades to less than 15% of its initial mass after 5 weeks in culture (15). To optimize extracellular matrix production and therefore mechanical properties at high pressures, we supplemented the culture medium with ascorbic acid, copper ion, and amino acids to support SMC collagen synthesis and cross-link formation (16, 17).

The vessels in Fig. 2, A through D, were grown in supplemented medium, whereas the vessel in Fig. 2, E and F was grown under pulsatile stress without culture medium supplementation. All vessels grown without supplementation displayed rupture strengths below 300 mm Hg. The specimen in Fig. 2E ruptured spontaneously at 270 mm Hg after 7 weeks of culture. In contrast, pulsed vessels cultured with medium supplementation ruptured at  $570 \pm 100$  mm Hg ( $n = 4$ ) after 5 weeks and at  $2150 \pm 709$  mm Hg ( $n = 3$ ) after 8 weeks. This

latter rupture strength is greater than that reported for native human saphenous veins [ $1680 \pm 307$  mm Hg, (5)] and is well within the range suitable for arterial grafting. Thus, supplemented medium was judged essential for vessel growth.

Table 1 summarizes the effects of pulsatile stress and increasing culture time on the characteristics of vessels grown in supplemented medium. Vessel wall thickness was increased both by increasing culture time and by pulsatile culture conditions and was comparable to native vessel wall thickness after 8 weeks in culture (18). The vessel collagen content (19) observed after 8 weeks of pulsatile culture conditions was 50% and was not significantly different ( $P < 0.1$ ) from that of native arteries (Table 1), whereas vessels grown without pulsatile stress possessed significantly ( $P < 0.005$ ) less collagen. Applied pulsatile stress significantly increased the observed suture retention strengths (20) after 5 ( $P < 0.001$ ) and 8 ( $P < 0.005$ ) weeks of culture to values as high as 90 g, which was still less than those observed for native arteries (Table 1).

Pulsatile culture conditions did not signifi-

cantly affect SMC density (21) ( $P < 0.1$ ), although these SMC densities are higher than those reported in systems where collagen gels are used as the matrix for SMC growth (22). The difference in calculated cell density between engineered and native vessels may be partly due to the volume occupied by polymer fragments in the engineered vessel wall.

Engineered vessels displayed measurable contractions in response to serotonin, endothelin-1, and prostaglandin  $F_{2\alpha}$ , the magnitudes of which were not affected by pulsatile culture conditions. Representative contractile forces in response to prostaglandin  $F_{2\alpha}$  ( $PGF_{2\alpha}$ ) are shown for five vessels (Fig. 3A). The measurable forces generated by these vessels ( $0.17 \pm 0.07$  g,  $n = 8$ ,  $P < 0.001$ ) after 8 weeks of cell culture demonstrate retained differentiated function, which is in contrast to the frequently observed loss of contractile phenotype by SMCs in vitro (23).

The mechanical behavior of the intact engineered vessels was further characterized by quantifying their stress-strain relationships. Vessels were subjected to a range of static intraluminal pressures, and magnified digital images of the vessels were obtained (24). The wall stress ( $\sigma$ ) and the midwall strain ( $\epsilon$ ) were calculated and plotted for six vessels (25) (Fig. 3, B and C). There was a linear relationship between the observed maximal incremental

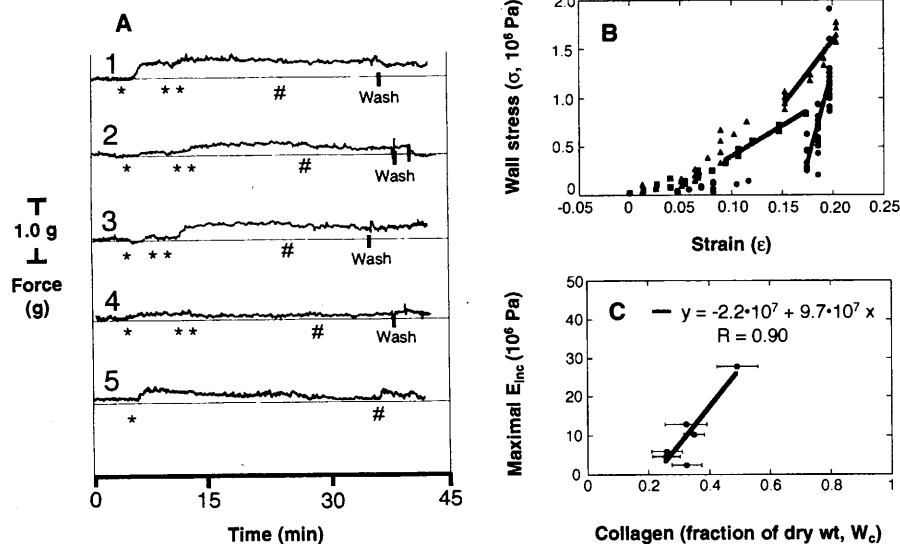


**Fig. 3.** (A) Pharmacological reactivity of engineered vessels (30). Segments of engineered vessel 2 mm in length were mounted on tungsten wires in conventional myographs. Rabbit abdominal aorta served as a control. Vessels were maintained at 4 g of tension for 30 min before testing and were treated with indomethacin ( $10^{-5}$  M) before constriction with prostaglandin  $F_{2\alpha}$  ( $PGF_{2\alpha}$ ). Absolute magnitudes of responses were approximately 5% of control vessels and 15% of reported values for excised vein grafts (31). 1 and 2, nonpulsed vessels cultured for 8 weeks; 3 and 4, pulsed vessels cultured for 8 weeks; 5, explanted xenograft in which contractile function is preserved. Single asterisk indicates  $PGF_{2\alpha}$ ,  $10^{-5}$  M; double asterisk indicates  $PGF_{2\alpha}$ ,  $10^{-4}$  M; number sign indicates papaverine,  $10^{-5}$  M. (B) Representative stress-strain plots for cultured vessels. External vessel diameters were extracted from the digital images, and vessel cross-sectional areas were obtained from analysis of fixed histologic sections. Circles, pulsed vessel cultured for 8 weeks; triangles, nonpulsed vessel cultured for 8 weeks; squares, pulsed vessel cultured for 5 weeks. Each data point represents a separate intraluminal pressure. At  $\sigma$  less than  $0.5 \times 10^6$  Pa, there was incomplete recruitment of collagen fibers (that is,  $f_c < 1.0$ ), and the value of  $E_{inc}$  was submaximal. At high stress levels, complete collagen fiber recruitment yields a maximal slope (solid lines) of the stress-strain relationship for each vessel and a maximal  $E_{inc}$ . (C) Maximal  $E_{inc}$  versus collagen content yields a linear relationship. The equation for the regression is shown. The value of the abscissa intercept, at  $W_c = 0.23$ , represents the minimum collagen content below which the mechanical properties of the engineered vessels would become negligible.

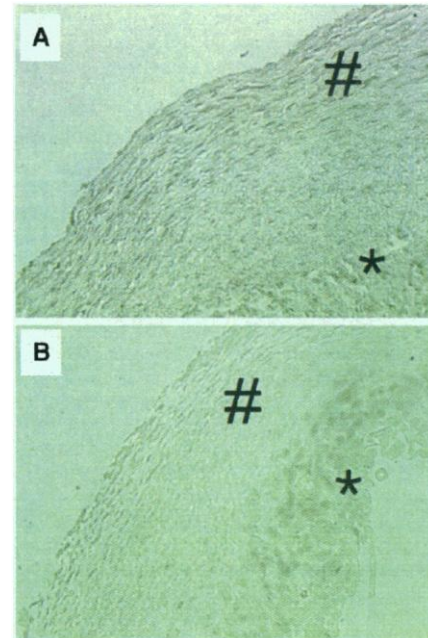


**Fig. 4.** Immunoperoxidase staining for myosin heavy chains. Number sign indicates the dense cellular region; asterisk indicates the polymer region. (A) Vessel cultured for 8 weeks with pulsatile stress. (B) Vessel cultured for 8 weeks without pulsatile stress. Myosin heavy chain staining was greater in the pulsed vessels and was observed in three sets of experiments. Nonspecific staining of polymer remnants is shown in (A) (orig. mag.  $\times 200$ ).

## REPORTS

modulus ( $E_{inc}$ ) at high wall stress and the collagen content [ $W_C$  (Fig. 3C)], with a correlation coefficient of  $R = 0.9$ . A linear relationship is expected and predicted from previous modeling of native vessels (13, 14, 25). From this relationship, we constructed a model that describes the incremental modulus of the vessel wall:  $E_{inc} = (9.7 \times 10^7 \cdot W_C - 2.2 \times 10^7) \cdot f_C$ , where  $f_C$  is the recruitment function for collagen fibers (13).

An ideal arterial conduit contains SMCs that are both contractile and quiescent with respect

to proliferation, decreasing the likelihood of SMC hyperplasia and consequent luminal occlusion after implantation (1). Immunoperoxidase staining for markers of SMC differentiation revealed that the SMCs of vessels grown under pulsatile or static conditions express significant amounts of smooth muscle  $\alpha$ -actin and calponin. However, the SMCs of vessels cultured under pulsatile conditions stained more intensely for myosin heavy chains, a late marker in ontological SMC development (23), as compared with nonpulsed vessels (Fig. 4, A and

B). In all vessels, the expression of these SMC markers was very low in regions containing polymer remnants.

Assessment of mitotic rate by immunohistochemical staining for proliferating cell nuclear antigen in the vessel wall revealed  $2.3 \pm 1.4\%$  positively staining SMC nuclei in the dense cellular region (Fig. 2B), as compared with  $19.4 \pm 9.6\%$  in the polymer scaffold region ( $P < 0.01$ ). Staining in the dense cellular region resembled that observed in the medial layers of native bovine and porcine vessels excised from young animals ( $3.7 \pm 0.6\%$ ). The application of pulsatile stress did not increase the mitotic rate in the dense cellular areas. However, the percent of stained SMCs in the polymer scaffold regions of endothelialized vessels was decreased to  $0.5 \pm 0.7\%$  ( $n = 2$ ,  $P < 0.01$ ), as compared with vessels that did not contain ECs. This result is consistent with the expected inhibition of replication of SMCs by confluent ECs (12) and would decrease the likelihood of SMC hyperplasia and vessel stenosis after implantation.

To assess the practical utility of these cultured arteries in vivo, we undertook initial implantation studies in four Yucatan miniature swine. Autologous arterial SMCs and ECs were cultured for each 6-month-old animal from small biopsies of the common carotid artery. For the first animal, a xenograft vessel that was cultured under pulsatile conditions from bovine arterial SMCs was seeded with autologous porcine arterial ECs 2 days before implantation. For the latter three animals, completely autologous grafts were cultured from carotid SMCs and ECs under conditions identical to those described for bovine cells, with the addition of platelet-derived growth factor BB (5 ng/ml) to the culture medium to promote SMC growth. Of the completely autologous grafts, one was grown under pulsatile conditions, and the remaining two were grown under static conditions.

All animals underwent implantation into the right saphenous artery, which is a branch of the femoral artery and is the largest artery in the distal half of the hindlimb. All animals were treated with daily aspirin (325 mg by mouth). Animals were followed for up to 4 weeks, after which time the grafts were explanted for assessment of histology and contractile function. All implanted vessels demonstrated good flow at implantation, and all grafts remained open for 2 weeks postoperatively as assessed by Doppler. The pulsed xenograft vessel was examined by digital subtraction angiography at 24 days after implantation and was patent, without evidence of stenosis or dilatation (Fig. 5A). The xenograft also had unchanged contractile responses to prostaglandin  $F_{2\alpha}$  (Fig. 3A) when explanted at 4 weeks (Fig. 5B). The pulsed autologous graft remained open for 4 weeks as assessed by Doppler, although decreased flow was noted at

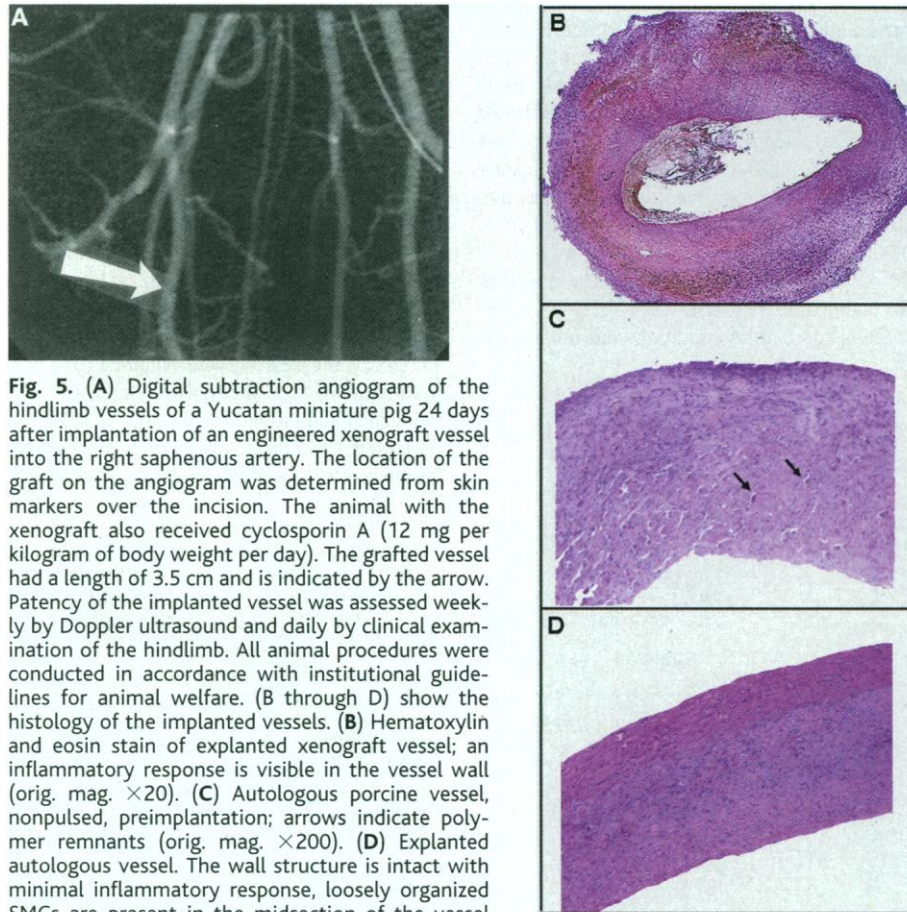


**Fig. 5.** (A) Digital subtraction angiogram of the hindlimb vessels of a Yucatan miniature pig 24 days after implantation of an engineered xenograft vessel into the right saphenous artery. The location of the graft on the angiogram was determined from skin markers over the incision. The animal with the xenograft also received cyclosporin A (12 mg per kilogram of body weight per day). The grafted vessel had a length of 3.5 cm and is indicated by the arrow. Patency of the implanted vessel was assessed weekly by Doppler ultrasound and daily by clinical examination of the hindlimb. All animal procedures were conducted in accordance with institutional guidelines for animal welfare. (B through D) show the histology of the implanted vessels. (B) Hematoxylin and eosin stain of explanted xenograft vessel; an inflammatory response is visible in the vessel wall (orig. mag.  $\times 20$ ). (C) Autologous porcine vessel, nonpulsed, preimplantation; arrows indicate polymer remnants (orig. mag.  $\times 200$ ). (D) Explanted autologous vessel. The wall structure is intact with minimal inflammatory response, loosely organized SMCs are present in the midsection of the vessel wall, and polymer remnants are no longer visible (orig. mag.  $\times 200$ ).

**Table 1.** Characteristics of engineered vessels.

Vessel type*	Wall thickness (cm)	Collagen (% dry weight)	Suture retention (g)	SMC density ( $10^8$ cells/ml)
5 P	$0.019 \pm 0.006$ ( $n = 4$ )	$29 \pm 6$ ( $n = 4$ )	$40 \pm 16$ ( $n = 4$ ) ( $P < 0.001$ )	$0.40 \pm 0.16$ ( $n = 4$ )
5 NP	0.009 ( $n = 1$ )	†	$2.7 \pm 1.2$ ( $n = 3$ )	†
8 P	$0.038 \pm 0.004$ ( $n = 5$ )	$50 \pm 5$ ( $n = 6$ ) ( $P < 0.005$ )	$91 \pm 26$ ( $n = 6$ ) ( $P < 0.005$ )	$0.93 \pm 0.37$ ( $n = 5$ )
8 NP	$0.023 \pm 0.004$ ( $n = 3$ )	$35 \pm 3$ ( $n = 4$ )	$22 \pm 8$ ( $n = 6$ )	$1.19 \pm 0.14$ ( $n = 3$ )
Native	0.029 (18)	$45 \pm 9$ ‡	$273 \pm 31$ ‡	$2.87 \pm 0.14$ §

\*P, pulsed; NP, nonpulsed; number represents weeks. †Data insufficient. ‡Measured from bovine muscular arteries stripped of adventitia. §Measured from bovine arteries by fluorometric assay.

the time of explantation. The mechanical strength of the explanted grafts could not be assessed accurately because of postsurgical fibroblast migration and collagen deposition at the outer surface of the engineered vessel.

In contrast, the two nonpulsed autologous grafts remained open for 3 weeks and then developed thrombosis, which may have been caused by gradual shearing loss of the luminal polymer region and of the endothelial layer due to arterial flows (Fig. 5, C and D). Histologically, the walls of the autologous explanted vessels showed highly organized structure and minimal inflammation as compared to the xenograft. For all vessels, there was no evidence of bleeding at the anastomoses or mechanical breakdown at explantation.

Important areas of future work include the effects of culture conditions on graft longevity, the stimulation of elastin in the vessel wall (26, 27), and the minimization of residual polymer fragments (28) in the engineered tissues. Clinically useful engineered vessels should approximate the patency rate of 90% at 30 days that is observed with autologous vein grafts (29). Although further studies are required to assess the biological function of these vessels during short-term and long-term implantation, the feasibility of culturing autologous implantable arteries and the important effects of pulsatile culture conditions have been demonstrated.

References and Notes

1. R. Ross, *Nature* **362**, 801 (1993).
2. J. V. Tu et al., *N. Engl. J. Med.* **336**, 1500 (1997).
3. R. D. Sayers, S. Raptis, M. Berce, J. H. Miller, *Br. J. Surg.* **85**, 934 (1998).
4. C. B. Weinberg and E. Bell, *Science* **231**, 397 (1986).
5. N. L'Heureux, S. Paquet, R. Labbe, L. Germain, F. A. Auger, *FASEB J.* **12**, 47 (1998).
6. W. Risau and I. Flamme, *Annu. Rev. Cell Dev. Biol.* **11**, 73 (1995).
7. G. K. Owens, *Circ. Res.* **79**, 1054 (1996).
8. P. F. Davies, *Physiol. Rev.* **75**, 519 (1995).
9. R. Ross, *J. Cell. Biol.* **50**, 172 (1971).
10. L. E. Niklason and R. S. Langer, *Transplant. Immunol.* **5**, 303 (1997).
11. J. Gao, L. E. Niklason, R. S. Langer, *J. Biomed. Mater. Res.* **42**, 417 (1998).
12. A. B. Dodge, X. Lu, P. A. D'Amore, *J. Cell. Biochem.* **53**, 21 (1993).
13. R. L. Armentano et al., *Am. J. Physiol.* **260**, H1870 (1991).
14. J. G. Barra et al., *Circ. Res.* **73**, 1040 (1993).
15. L. E. Freed et al., *Bio/Technology* **12**, 689 (1994).
16. J. M. Davidson, P. A. LuValle, O. Zoia, D. Quaglino, M. G. Giro, *J. Biol. Chem.* **272**, 345 (1997).
17. D. Tinker and R. B. Rucker, *Physiol. Rev.* **65**, 607 (1985).
18. C. G. Caro, T. J. Pedley, R. C. Schroter, W. A. Seed, *The Mechanics of the Circulation* (Oxford Univ. Press, Oxford, 1978).
19. J. F. Woessner, *Arch. Biochem. Biophys.* **93**, 440 (1961).
20. Association for the Advancement of Medical Instrumentation (AAMI), *American National Standard for Cardiovascular Implants-Vascular Prostheses* (American National Standards Institute (AAMI, Arlington, VA, 1994).
21. Y. J. Kim, R. L. Sah, J. Y. H. Doong, A. J. Grodzinsky, *Anal. Biochem.* **174**, 168 (1988).
22. T. Ziegler and R. M. Nerem, *J. Cell. Biochem.* **56**, 204 (1994).

23. G. K. Owens, *Physiol. Rev.* **75**, 487 (1995).
24. G. J. L'Italien et al., *Am. J. Physiol.* **267**, H574 (1994).
25. The wall stress ( $\sigma$ ) was calculated from (13, 14) as follows:

$$\sigma = 8 \cdot P \cdot (r_e r_i)^2 / [(r_e^2 - r_i^2) \cdot (r_e + r_i)^2] \quad (1)$$

where  $r_e$  is the measured external radius,  $r_i$  is the internal radius calculated from the measured external radius and cross-sectional area, and  $P$  is the intraluminal pressure. Wall strain ( $\epsilon$ ) was calculated at the midwall radius as follows:

$$\epsilon = [(r_e + r_i)/2] / [(R_e + R_i)/2] - 1 \quad (2)$$

where  $R_e$  and  $R_i$  are the external and internal vessel radii under unstressed conditions (at  $P = 25$  mm Hg) (13, 14). The formulation for  $E_{inc}$  is based on models previously reported to describe native vessels (elastin staining in engineered vessels was negative, so elastin is neglected) (13, 14):

$$E_{inc} = E_C W_C f_C + E_{SM} W_{SM} \quad (3)$$

where  $E_{inc}$  is the incremental modulus, calculated from the slope of the stress-strain curves (Fig. 3B);  $E_{inc} = 0.75(d\sigma/d\epsilon)$ ;  $E_C$  and  $E_{SM}$  are elastic moduli for collagen and SMCs, respectively;  $W_C$  and  $W_{SM}$  are amounts of collagen and SMCs in the vessel wall; and  $f_C$  is the recruitment function for collagen. The re-

cruitment function describes the fraction of total collagen fibers that support wall stress at a given strain. Previously reported values of maximal  $E_C \cdot W_C$  fall in the range of  $1.3 \pm 0.6 \times 10^8$  Pa. From Fig. 3A, we calculate the maximal SMC-supported wall stress for any vessel to be approximately  $6 \times 10^3$  Pa. This negligible SMC contribution effectively reduces the model to a function of the collagen content alone.

26. D. Y. Li et al., *Nature* **393**, 276 (1998).
27. S. K. Rao, K. V. Reddy, J. R. Cohen, *Ann. N.Y. Acad. Sci.* **800**, 131 (1996).
28. H. P. Greisler, C. Gosselin, D. Ren, S. S. Kang, D. U. Kim, *Biomaterials* **17**, 329 (1996).
29. J. L. Cox, D. A. Chiasson, A. I. Gottlieb, *Progr. Cardiovasc. Dis.* **34**, 45 (1991).
30. W. Steudel et al., *Circ. Res.* **81**, 34 (1997).
31. K. S. Cross et al., *Br. J. Sur.* **81**, 699 (1994).
32. We thank J. Bevan for assistance with the contractile function testing and P. D'Amore for helpful discussions. This work was supported by National Heart, Lung and Blood Institute grant K08HL03492, NIH grant HL60435, and the Foundation for Anesthesia Education and Research.

11 January 1999; accepted 18 March 1999

## Dense Populations of a Giant Sulfur Bacterium in Namibian Shelf Sediments

H. N. Schulz,<sup>1\*</sup> T. Brinkhoff,<sup>2</sup> T. G. Ferdelman,<sup>1</sup> M. Hernández Mariné,<sup>3</sup> A. Teske,<sup>4</sup> B. B. Jørgensen<sup>1</sup>

A previously unknown giant sulfur bacterium is abundant in sediments underlying the oxygen minimum zone of the Benguela Current upwelling system. The bacterium has a spherical cell that exceeds by up to 100-fold the biovolume of the largest known prokaryotes. On the basis of 16S ribosomal DNA sequence data, these bacteria are closely related to the marine filamentous sulfur bacteria *Thioploca*, abundant in the upwelling area off Chile and Peru. Similar to *Thioploca*, the giant bacteria oxidize sulfide with nitrate that is accumulated to  $\leq 800$  millimolar in a central vacuole.

Filamentous, nitrate-accumulating sulfur bacteria of the genus *Thioploca* form extensive populations of up to 120 g wet weight/m<sup>2</sup> along the coast of Chile and Peru (1-3). Similar to the South American continental shelf, the shelf off Namibia has strong upwelling with high plankton productivity and oxygen-depleted bottom water (4). In a search for *Thioploca* along the Namibian coast, we obtained sediment samples from water depths of ~100 m during a cruise in April 1997 aboard the R/V Petr Kottsov. *Thioploca* and its close relative *Beggiatoa* were present, but only in low numbers. Instead, we

discovered large populations of a previously undescribed sulfur bacterium that occurred at biomasses of up to 47 g m<sup>-2</sup>. These giant bacteria grow as a string of pearls, which shine white because of refractive sulfur globules and are large enough to be visible to the naked eye (Fig. 1A). We suggest the genus and species name *Thiomargarita namibiensis*, "Sulfur pearl of Namibia," for this organism.

*Thiomargarita* was found at stations between Palgrave Point and Lüderitz Bay. The highest biomasses were between Cape Cross and Conception Bay. The surface sediment in this area is a fluid, green diatom ooze (5). Oxygen concentrations were low, 0 to 3  $\mu$ M, in the overlying water at all stations, whereas nitrate was present at 5 to 28  $\mu$ M. Sulfate reduction rates measured by the <sup>35</sup>SO<sub>4</sub><sup>2-</sup> tracer technique were high, 14 to 76 mmol m<sup>-2</sup> day<sup>-1</sup> in the upper 19 cm, and gave rise to high sulfide concentrations of 100 to 800  $\mu$ M in the upper 3 cm of the sediment. Frequently, the water directly overlying the sediment smelled of sulfide. Most of the bacteria were found in the top

<sup>1</sup>Max Planck Institute for Marine Microbiology, Celsiusstrasse, D-28359 Bremen, Germany. <sup>2</sup>Institute for the Chemistry and Biology of the Marine Environment (ICBM), University of Oldenburg, Post Office Box 2503, D-26111 Oldenburg, Germany. <sup>3</sup>Facultat de Farmàcia, Universitat de Barcelona, Av. Joan XXIII, s/n, 08028 Barcelona, Spain. <sup>4</sup>Department of Biology, Woods Hole Oceanographic Institution (WHOI), Woods Hole, MA 02543, USA.

\*To whom correspondence should be addressed. E-mail: hschulz@mpi-bremen.de